Annual Journal of Hydraulic Engineering,
JSCE VOL. 41 (1997)

VORTEX CONVECTION GENERATED BY A V-SHAPED OBSTRUCTION IN STRATIFIED FLOW

By PHAM Hong Son* Takashi ASAEDA** and Masamitsu ARITA***

ABSTRACT: Strong vortex convection can be generated by placing a V-shaped plate in a horizontal flow. Experimental investigation was conducted in linear stratified flow under variation of Reynolds number *Re*, Richardson number *Ri* and dihedral angle of the V-plate. It was found that the maximum vortex rising height can be attained with a dihedral angle of about 90°. Large eddy simulation model with non-uniform mesh and non-staggered grid scheme was used to study the flow structure that shed from the plate. Experimental and numerical results conclude that the rising height of produced vortices may reach 6 times the plate height and weakly depends on Reynolds number in homogeneous flow. It has reduced in stratified flow to 4 times of the plate height with Ri =0.12 and smaller than 3 times with Ri larger than 0.4. The simple V-shaped structure efficiently generated upwelling current that can be used as mixing for environment purpose

Keywords: vortex, upwelling current, mixing, large eddy simulation.

1. INTRODUCTION

In its' natural and unpolluted state deep estuarine water is rich in nutrients, such as phosphorous and nitrate salts, in a suitable ratio to sustain marine life. If such a source of nutrients can be convected to the surface layer, where most of the biological production in the ocean occurs, it can be expected to promote the growth of plants and fish in that region (Marino Forum 1990, Asaeda et al. 1991). In certain situations however the deep water can stagnate and become eutrophic. In this case the advantage of rising the deep water to the surface is that it can receive oxygen, thus preventing eutrophication. It is thus apparent that a passive, efficient means of raising deep water to the surface would be an invaluable tool for preserving and improving aquatic environments.

Asaeda et al. (1989) observed a strong upward current along the slope of the trailing ridge of a three-dimensional sand ripple. They stressed the fact that the strong current was caused by a horse-shoe vortex and intensified by the three-dimensional configuration of the ripples. It was found that a converging trailing ridge holds a key to the formation of strong rising current because of it's inherent production of the horse-shoe shape vortex. Based on this study it was concluded that a symmetrical V-shaped plate in plan with finite height, placed with the bend of the V facing downstream, should be further investigated.

Asaeda et al. (1994) experimentally and numerically investigated the structure of vortices that shed from V-shaped dihedral angle plate in homogeneous horizontal flow. They found that the produced vortices coalesce with neibouring ones to form stronger vortices and moved upward. Here, more detailed vortex structures were simulated with LES model.

* Grad. Student, Dept. of Environmental Sciences, Saitama Univ.
(255 Shimo-okubo, Urawa, Saitama 338)
** Assoc. Prof., Dept. of Environmental Sciences, Saitama Univ.
(255 Shimo-okubo, Urawa, Saitama 338)
*** Professor, Dept. of Construction Engrg., Tokyo Denki University
(Hatoyama, Saitama, 350-03)

2. EXPERIMENTAL STUDY.

The experiment was performed in a flume of 8m long and 0.42m wide. A salt water with 40cm deep and linear density variation was contained in the flume to serve as a stratified environment (see figure 1). The density of the water on the surface was 1.0 g/cm^3 while at the bottom the water was heavier with the density of 1.00, 1.02, 1.04 and 1.06 g/cm^3 varying in each run. To ensure the linear density profile in the flume the vertical density distribution was measured before the experiments.

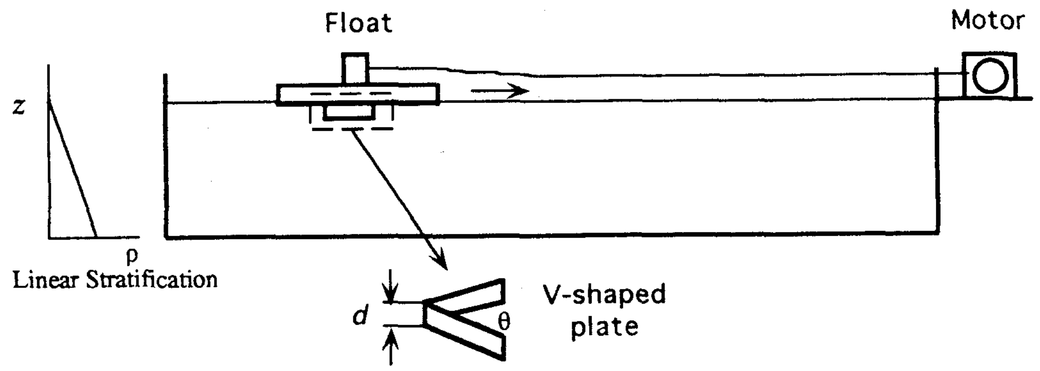

Figure 1. Experimental facility

A V-shaped dihedral plate of 2cm high, with each branch of 10cm long was placed downward on the bottom of a float, which initially located near the one end of the flume. The float can move steadily along the flume by a motor placing on the other end with the help of a connected string. The V-shaped dihedral plate was placed so that their opened branches against the water when the float in motion. The main velocity in the experiments, which can be regulated by the motor, was 2.3, and 6.7cm/s. The Reynolds number *Re* was defined base on the main velocity *U*, the plate height d and the kinematic viscosity. The Richardson number R_i was defined as

$$R_i = \frac{d\rho}{\rho_r dz}\frac{gd^2}{U^2} \quad (1)$$

where ρ is density and ρ_r is the reference density.

Flow patterns were visualised by injecting dye (water blue) loading on the float from three injection pipes mounted at both ends and at the center of the plate. As the float moves along the flume, the dye injected and thus the flow patterns behind the plate can be clearly observed. The experiments were carried out for 8 flow conditions with the difference in Richardson numbers and Reynolds numbers. In each flow condition the dihedral angle θ was varied from 30° to 180° with increments of 30° for each measurement. Experimental conditions are listed in table 1.

Table 1. Experimental Condition

Run (1)	Average Velocity U (cm/s) (2)	Reynolds Number *Re* (3)	Density at bottom (g/cm^3) (4)	Richardson Number *Ri* (5)	Dihedral angle of V-plate θ (degrees) (6)
1	6.7	1020	1.00	0.000	30, 60, 90, 120, 150, 180
2	2.3	340	1.00	0.000	30, 60, 90, 120, 150, 180
3	6.7	1020	1.02	0.043	30, 60, 90, 120, 150, 180
4	2.3	340	1.02	0.394	30, 60, 90, 120, 150, 180
5	6.7	1020	1.04	0.087	30, 60, 90, 120, 150, 180
6	2.3	340	1.04	0.788	30, 60, 90, 120, 150, 180
7	6.7	1020	1.06	0.131	30, 60, 90, 120, 150, 180
8	2.3	340	1.06	1.182	30, 60, 90, 120, 150, 180

3. FLOW PATTERNS

Figure 2 shows typical flow patterns which were taken by a camera (run 5). It is supposed that the structure of the flow obtained in the experiments is similar to those which would be produced by placing a V-shaped dihedral plate at the bottom of the channel. An observation showed that the structure of the flow just behind the plate is similar to the case of the homogeneous flow which reported in Asaeda et al (1994). The vortices produced by the flow passing around and over the edges of the plate coalesces and was affected by bottom to form a vortex. After being created, however, vortex is strongly affected by the stratification of the environment. Since vortices were formed near the channel bottom, they were heavier than the water on higher level. The self-induced upward motion of produced vortices, therefore, was being pushed downward. Consequently, the rising height of vortices is reduced depending on flow condition.

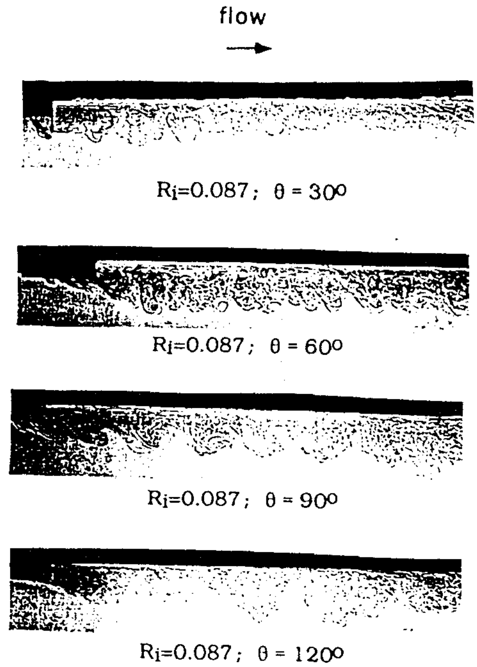

Figure 2. Observed Flow Patterns

4. NUMERICAL SIMULATION

The large eddy simulation (LES) was selected for present development. The filtered Navier-Stokes equations, continuity equation and equation of density transfer in incompressible flow may be written in Cartesian tensor form as

$$\frac{\partial \bar{u}_i}{\partial t} + \frac{\partial}{\partial x_j}(\bar{u}_i \bar{u}_j) = -\frac{\partial \bar{p}}{\partial x_i} + \frac{\partial}{\partial x_j}\left(2\nu \bar{S}_{ij} - \tau_{ij}\right) - \frac{\bar{\rho} - \rho_r}{\rho_r} g\delta_{i3} \tag{2}$$

$$\frac{\partial \bar{u}_j}{\partial x_j} = \bar{S}_{ii} = 0 \tag{3}$$

$$\frac{\partial \bar{\rho}}{\partial t} + \frac{\partial}{\partial x_k}(\bar{u}_k \bar{\rho}) = \frac{\partial}{\partial x_k}\left(\alpha \frac{\partial \bar{\rho}}{\partial x_k} - q_k\right) \tag{4}$$

where the overbar denotes the filtering operation, u_i are the filtered velocity components in three directions, t is time, p is pressure, ρ is filtered density, ρ_r is reference density , τ_{ij} are the subgrid scale (SGS) Reynolds stress, g is gravity acceleration, δ_{ij} is Cronecker delta, ν is the molecular viscosity and α is diffusivity. The filtered strain rate tensor is defined by

$$\bar{S}_{i,j} = \frac{1}{2}\left(\frac{\partial \bar{u}_i}{\partial x_j} + \frac{\partial \bar{u}_j}{\partial x_i}\right) \tag{5}$$

The stress tensor τ_{ij}

$$\tau_{i,j} = \overline{u_i u_j} - \bar{u}_i \bar{u}_j \tag{6}$$

and the residual density flux

$$q_k = \overline{\rho u_k} - \overline{\rho}\,\overline{u}_k \tag{7}$$

must be modelled

The Smagorinsky model which approximated the SGS Reynolds stress as

$$\tau_{ij} - \frac{1}{3}\delta_{ij}\tau_{kk} = -2\nu_t \bar{S}_{ij} \tag{8}$$

is untilized where the turbulent viscosity ν_t is

$$\nu_t = C\Delta^2|\overline{S}|. \tag{9}$$

An analogous eddy diffusivity model (Eidson 1985, Zang 1990)

$$q_k = -\alpha_t \frac{\partial \overline{\rho}}{\partial x_k} \tag{10}$$

where

$$\alpha_t = C_p \Delta^2 |\overline{S}|, \tag{11}$$

$$|\overline{S}| = |\overline{S}_{ij}\overline{S}_{ij}|^{1/2}, \tag{12}$$

Δ is filter width equals the grid size and coefficient C=0.2, C_p=C/Pr_t (Pr_t is SGS turbulent Prandtl number) was applied.

The equations (2-4) are then made dimensionless by velocity scale $\overline{U}$ which taken as entrance main velocity of the channel, length scale H taken as depth of channel (vertical size of computational domain), density by reference density (density of fresh water) and time by $H/\overline{U}$.

A region of the channel with dimension of 1m long (10 times the branch of the plate or 50 times the plate height), 0.4m width (4 times the plate branch or 20 times the plate height) and 0.2m depth (10 times the plate height) was set for simulation. A limit of our computer capacity and its speed did not allow us to compute for larger domain. According to experimental observation the computational domain is sufficient in relation to the plate size for development of the expected flow and it is believed that boundary will not effect in the flow structure.

To construct the mesh a series of zoned meshes initially constructed. The smallest grid size in finest zone nearest the V-shaped plate was 0.0025m in all three directions. They are gradually increased in the coarest zone to 0.0107m in horizontal direction and 0.00665m in surface.

The equations then are discretized on non-staggered mesh in finite difference form with second order centred space differences for all viscous-like terms (including the SGS terms), and the pressure gradient and divergence terms. Armfield (1991) proposed a finite difference scheme for solving the Navier-stokes equation on a non-staggered mesh that preserves the features of the SIMPLE scheme. The method of ensuring strong ellipticity of the discrete equation, by the addition of a term to the continuity equation, designated the elliptic pressure term. The additional terms included are of the same order and smaller magnitude than the leading order truncation error of the discrete continuity equation, and thus do not adversely affect the accuracy of the solution. The sequence in which the equations are solved and the convergence calculation is the same as that given in Armfield (1991). We choose this scheme to construct the model in present study.

A constant normal velocity with 1/7 power law distribution near the bottom region, zero tangential velocity, zero vertical velocity and linear density distribution is specified at the entrance. It is assumed that there is zero velocity gradient and zero density variation in the normal direction at the exit. Zero velocity gradient and zero density variation in tangential direction were imposed at both side boundaries. Zero velocity gradient and zero density variation in vertical direction were specified at upper boundary. Zero velocity and zero gradient density were imposed at bottom, and V-shaped plate body. Pressure is obtained by a second order extrapolation from the interior on the all boundaries, while the normal gradient of the pressure correction is set to zero on all the boundaries to allow the Poisson pressure correction equation to be solved.

Zero tangential and vertical velocities were imposed at initial computation. The normal velocity with 1/7 power law distribution was specified for whole channel excluded the V-shaped body in which zero velocity was imposed. At beginning the linear density distribution was given.

5. NUMERICAL RESULTS

The numerical study began with calculation for a set of flow condition U=0.067m/s, $\Delta\rho$=0 (homogeneous fluid), θ=90°. It was found that it was better to calculate with time step Δt=0.001. With larger Δt the stability was hardly achieved while with smaller Δt a lot of time was required for calculation. At beginning stage, the computation was hard to converge. Once the several initial steps were over the interactions were converged with the convergence criterion being the requirement that the mean residual of the continuity equation was less than 0.001. The computed results at step 22000 (t=22 s) were taken for analyses. The side view of the flow structure was given in figure 3(a) at y/d=1.25 and the cross section view of the channel was given in figure 3(b) at a distance behind the plate x/d=4.0. In these figures the lengths were in nondimensional form corresponding to the plate height d, x, y, z were lengths in normal direction, in tangential direction and in vertical direction respectively. The axis base was the point located in inner side of the head of the V-shaped plate and at bottom of the channel. A triangular separation zone was formed behind the plate, containing strong recirculation as a result of the vorticity shed from the flow passing over the plate, which will subsequently be called the surmounting flow. The flow passing around the edges of the plate produced a strong vortex with axis aligned perpendicular to the floor, originating from the bottom at the lee- side of the plate end. The two vortices originating at either end of the plate then join with the other vortices produced by the surmounting passing over the upper edge of the plate to form a stronger vortex. After shedding, the vortex head, that is the center region of the V-shaped vortex, was pushed upward by both the surmounting flow and the horizontally converging flow in the wake. Both branches were then stretched in the streamwise direction and forced to approach each other by the bottom effect.

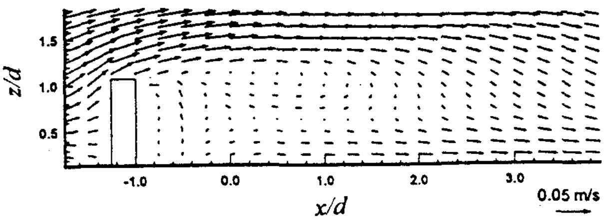

(a)

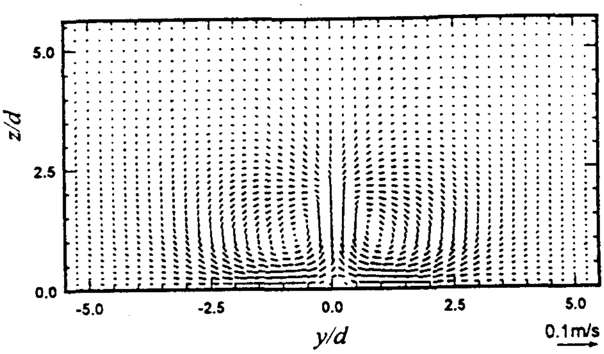

(b)

Figure 3. Vortex structure near the V-plate flow
(a) side view, (b) cross view

The calculation then carried out for a set of flow condition U=0.067m/s $\Delta\rho$=0 and different dihedral angle θ=30°, 60°, 120°, 150°. One selected centerline side view of obtained flow is shown in Figure 4. As already noted previously, the upward currents behind the plate can be observed for all cases, among which the strongest current was achieved with θ=90°.

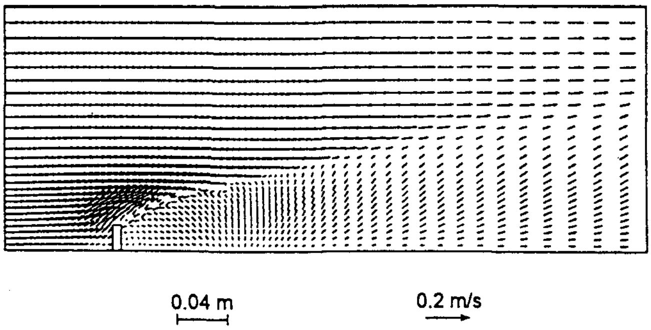

Figure 4. Calculated centerline side view of flow behind the V-plate
Run 1, θ=90°, Re=1020

The obtained results for different dihedral angle with regard to the Richardson number were sketched in the figure 5 together with experimental results. The rising height of the vortex head was largest with the dihedral angle of 90° and reduced with increasing Richardson number. It reached 6 times the plate height in homogeneous fluid and about 4-5 times with *Ri* less than 0.087 (runs 3 and 5). For higher R_i this height was only 2-3 times (runs 4,6,7). In the case of very high R_i (run 8), the produced vortices were very weak.

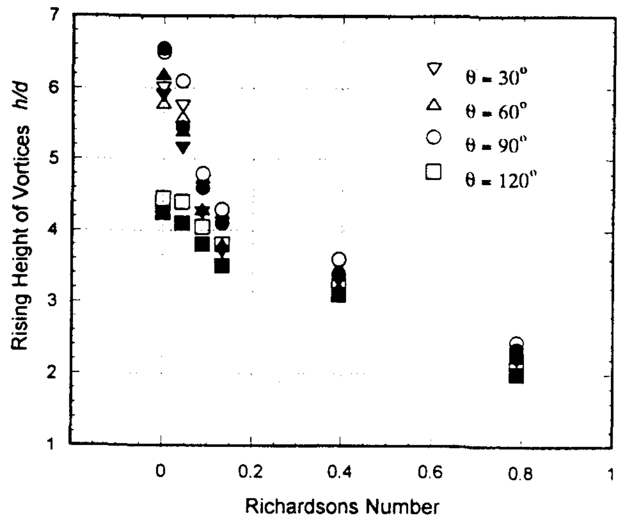

$$R_i = \frac{d\rho}{\rho_r \mathrm{d}z}\frac{gd^2}{U^2}$$

Figure 5. Rising height of vortex in terms of *Ri* at *x/d*=20,
Open marks: Experimental results,
Full marks: Calculated results.

6. CONCLUSION

Experimental and numerical results show that the vortex wake behind the V-shaped plate is closely related to a number of factors.

The formation of vorticies directly depends on the angle of attack which equals half of dihedral angle of the plate θ. The strongest upward vortex is obtained with θ is about 90°.

The optimal rising height of the vortex can be reached 6 times the plate height in the homogeneous environment. However, it reduces in the stratified fluid with the increasing of the Richardson number. This height was about 4-5 times the plate height *d* with R_i=0.012 and smaller than 3 times with R_i larger than 0.4.

Apparently the 90° dihedral V-shaped structure is a simple and efficient means of generating an upward rising current. Such a structure may be of practical application in regions with currents and small Richardson number that require mixing for environmental reasons.

REFERENCES

1) Asaeda, T., Nakai, M., Manandhar, S.K. and Tamai, N., (1989), Sediment entrainment in channel with rippled bed. J. Hydr. Engrg., ASCE, 115, 327-339.
2) Asaeda, T., Pham H., S., Armfield, S., (1994), Vortex convection produced by V-shaped dihedral obstruction. J. Hydr. Engrg. ASCE, 120 (11), 1274-1291.
3) Armfield S.W., (1991), Finite difference solutions of the Navier-Stokes equations on staggered and non-staggered grids, Computer Fluids. Vol. 20, No. 1, pp 1-17.
4) Galperin B., Orszag S. A., (1993), Large Eddy Simulation of complex engineering and geophysical flows, Cambridge University Press.
5) Patankar, S.V., (1980) Numerical heat transfer and fluid flow, Hemisphere Publishing Corporation.